Hybrid Materials

DOI: 10.1002/anie.200900554

Mechanical Nanosensor Based on FRET within a Thermosome: Damage-Reporting Polymeric Materials**

*Nico Bruns, Katarzyna Pustelny, Lisa M. Bergeron, Timothy A. Whitehead, and Douglas S. Clark**

The emerging interface of biology and materials science is creating new opportunities for the design, synthesis, and optimization of biologically enabled and biologically inspired materials. The incorporation of proteins into polymers can result in hybrid materials that combine the properties of the polymer as a cost-effective and easily processable material with the highly evolved biological functionality of the protein, which enables new concepts for the construction of sensors, biomedical materials, and drug-delivery systems.[1] Specific examples include biocatalytic polymers[2] and detoxification foams[3] that combine the catalytic properties of enzymes with the structural properties of polymers. Furthermore, hydrophilic polymers have been cross-linked with proteins to generate hydrogels that alter their swelling state due to conformational changes of the protein in response to an external stimulus such as a change in temperature[4] or the presence of a ligand.[5] Protein-crosslinked hydrogels have also been developed that are biodegradable[6] or incorporate the pH- and temperature-dependent fluorescence of the green fluorescent protein into the gel.[6b]

A common feature of these materials is that the functionality of the biomolecule is added to, and alters the properties of, the polymer. However, to the best of our knowledge, the reverse situation, in which changes in the polymer alter the properties of the protein, has not been reported to date. Such a scenario is essential in order to create self-reporting hybrid materials, where proteins are used as reporter molecules that sense deformation, strain, or mechanical damage in materials. Self-reporting materials are an intriguing possibility for the detection of internal damage before occurrence of catastrophic failure of the material.[7] The early detection of impending failure is especially important in cases where the polymer is used as a load-bearing material (e.g., fiber-reinforced polymer composites in automotive and aerospace applications), as a polymer adhesive, or as a material that comes into contact with liquids (e.g., tubing, biomedical materials) and can warn against potential leakage.

Herein, we present the concept of a protein-based nanosensor that is able to report deformation of the embedding polymer matrix. We combined the structural properties of the thermosome (THS), a chaperonin from the thermophilic organism *Thermoplasma acidophilum*, with the spectral properties of fluorescent proteins to generate a protein complex that exhibits fluorescence resonance energy transfer (FRET) and is sensitive to structural deformation (Figure 1).

THS is a spherical, hexadecameric complex consisting of two stacked, eight-membered rings that join at the equatorial plane of a spherical structure (Figure 2a).[8] This plane is the mechanically weakest part of chaperonins.[9] Each ring forms a half sphere, is composed of alternating α and β subunits with a molecular weight of 58 kDa, and encloses a central cavity with a diameter of approximately 5 nm and a void volume of 130 nm^3. Each cavity is large enough to accommodate globular proteins of approximately 45 kDa.[8] In contrast to the GroEL–GroES complex from *E. coli*, which is the most widely studied chaperonin,[10] both rings of THS have a built-in lid formed by helical protrusions at the tip of the apical domain of each subunit. These lids can open and close in an adenosine triphosphate (ATP) dependent manner.

Our concept for a THS-based stress sensor is shown in Figure 1. It is based on the idea that guest proteins can be permanently entrapped into the cavities by covalent linker chemistry. Entrapping a donor–acceptor pair of fluorescent proteins into the cavities gives the possibility for FRET to occur. The centers of the two cavities are approximately 7 nm apart, which is close to the Förster radius (4.9 nm) of enhanced cyan fluorescent protein (eCFP) and enhanced yellow fluorescent protein (eYFP),[11] which are the most commonly used donor–acceptor FRET pair in molecular biology.[12] We thus hypothesized that, by covalently cross-linking chains of a polymer matrix with the THS–guest complex, a sufficient force applied to the matrix will separate the two halves of the THS, which results in reduced FRET (Figure 1a). Another possible reporting mechanism, whereby a separated THS complex relaxes back to its native conformation because of stress relaxation around the cracks, thus

[*] Dr. N. Bruns,[+] K. Pustelny, Dr. L. M. Bergeron, Dr. T. A. Whitehead, Prof. D. S. Clark
Department of Chemical Engineering, University of California
201 Gilman Hall, Berkeley, CA 94720 (USA)
Fax: (+1) 510-643-1228
E-mail: clark@berkeley.edu
Homepage: http://www.cchem.berkeley.edu/clarkgrp/

[+] Current address: Dept. of Chemistry
University of Basel (Switzerland)

[**] We are indebted to Prof. Jeffrey Urbach (Georgetown University) for helpful discussions and assistance in preparing the manuscript. We are grateful to Prof. Anthony R. Clarke and Dr. M. Giulia Bigotti (School of Medical Sciences, University of Bristol (UK)) for a gift of the plasmid that encodes the native THS. We thank Holly L. Aaron at the Berkeley Molecular Imaging Center for assistance with the confocal and FLIM microscopy, as well as Prof. Jean M. Fréchet and Prof. Carolyn R. Bertozzi for the use of their instrumentation. The research described in this article was funded by the Air Force Office of Scientific Research (FA9550-07-1-0116). FRET = fluoresence resonance energy transfer.

Supporting information for this article is available on the WWW under http://dx.doi.org/10.1002/anie.200900554.

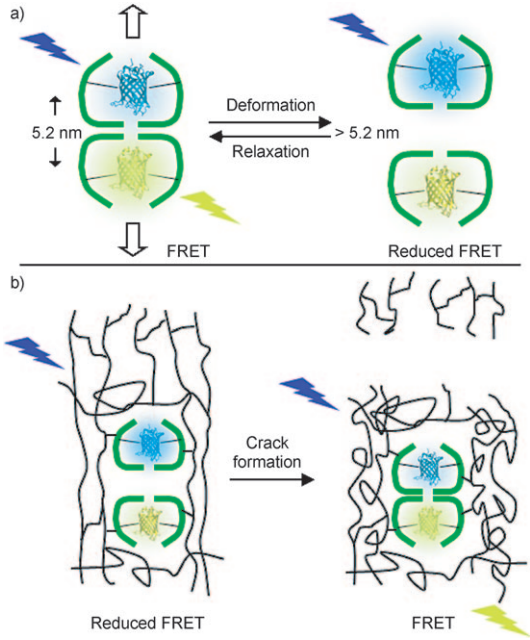

Figure 1. Concept of a reporter for structural deformation comprising a FRET pair of fluorescent proteins coencapsulated into the two cavities of the thermosome (THS). eCFP and eYFP can serve as donor and acceptor species for FRET, and the dimensions of the THS complex will position these variants in separate cavities within the required distance (Förster radius = 4.9 nm). a) Deformation of the complex increases the distance between the fluorescent proteins, resulting in a reduced FRET process. b) In this system, THS is covalently incorporated into a glassy polymeric network. Internal stress within this hybrid material leads to deformation of the THS native structure and cavity separation. Upon formation of cracks, the polymer and THS in the vicinity of a crack relaxes, which can be detected by changes in the emission intensity of the FRET acceptor.

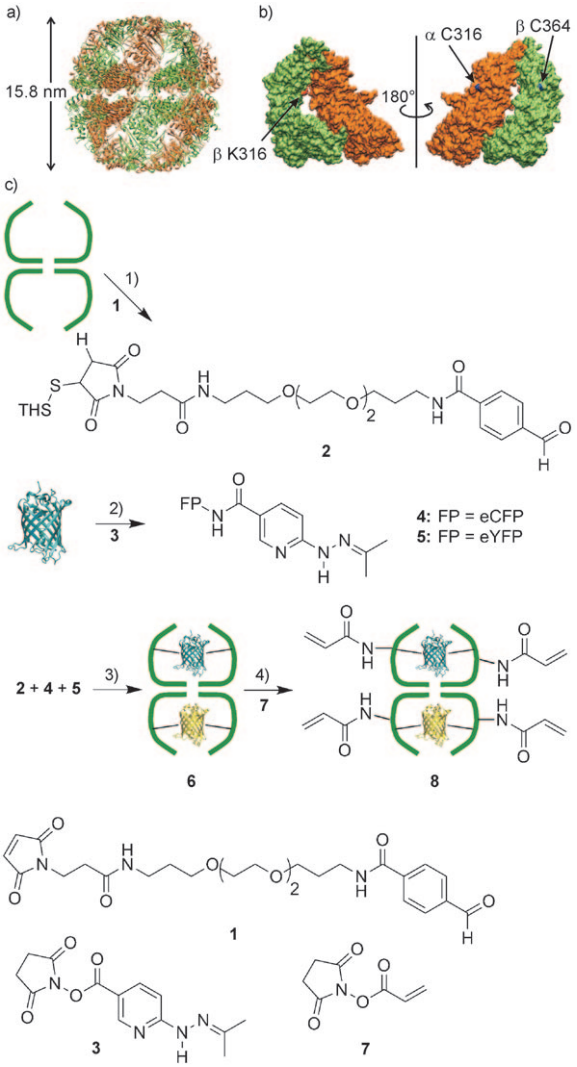

Figure 2. Structure of THS and strategy to covalently entrap fluorescent proteins into the chaperonin. a) Side view of THS in its closed conformation.[8] b) Surface representation of one α and β subunit, showing the targets of the three point mutations that were chosen to introduce a cysteine residue inside the cavity and to remove exposed cysteine residues on the external surface. c) Coupling chemistry used to covalently bind fluorescent proteins into the cavities of THS and yield THS-eCFP-eYFP (**6**). Further modification of the protein's lysine residues with **7** introduced copolymerizable acrylamide groups. 1) [THS] = 2.0 mg mL^{-1}, [**1**] = 442 μM, sodium phosphate buffer (100 mM, pH 6.5, 150 mM NaCl); 2) [FP] = 1.0 mg mL^{-1}, [**3**] = 313 μM, sodium phosphate buffer (100 mM, pH 7.4, 150 mM NaCl); 3) [**2**] = 2.0 mg mL^{-1}, [**4**] = [**5**] = 1.76 mg mL^{-1}, 1,3-bis-(tris(hydroxymethyl)methylamino)propane (bis-tris-propane) buffer (100 mM, pH 6.5, 150 mM NaCl); 4) [**6**] = 1.0 mg mL^{-1}, [**7**] = 355 μM, sodium phosphate buffer (100 mM, pH 7.4, 150 mM NaCl).

resulting in increased FRET in the vicinity of the cracks compared to the nonrelaxed matrix, is shown in Figure 1b.

To construct the sensor, specific chemical attachment points had to be engineered into the cavities of the THS complex. To this end, three site-directed mutations were carried out simultaneously. The mutation K316C in the β subunit introduced cysteine residues into the wall of each cavity (Figure 2b). However, the native THS has one surface-exposed cysteine on the outside of each subunit, which was replaced by alanine. As a fully assembled THS is built of two eight-membered rings with alternating α and β subunits, its engineered form exposes four cysteine groups in each cavity and none on its outer surface, thus allowing the selective coupling of protein guests inside the cavities.

The genes of the genetically engineered α and β subunits were co-expressed in tandem in a pET-27b vector in the host-cell line *E. coli* BL21(DE3) Codon Plus-RIL by following a protocol described for the native THS.[13] Fermentations were carried out in the nutrient-rich medium Terrific Broth at 30 °C (see the Supporting Information). THS was purified from the soluble cell extract in three steps. Initial anion-exchange chromatography was followed by size-exclusion chromatography to yield a high-molecular-mass species. This fraction was then subjected to a second, high-resolution anion-exchange step to separate fully assembled α_8/β_8 THS from assemblies that contained mismatched α and β subunits. Fractions with a 1:1 ratio of α and β subunits were identified by sodium dodecyl sulfate polyacrylamide gel electrophoresis (SDS-PAGE) and combined. Nondenaturing native PAGE revealed one band corresponding to a species with a molecular mass of approximately 960 kDa and was attributed

to the fully assembled THS. The overall yield of the chaperonin was 12 mg protein per liter of culture.

The guest proteins eCFP and eYFP were entrapped within the cavities of the thermosome by covalent coupling between the cysteine residues in the cavities and surface-exposed lysine groups of the guests. The linker chemistry is shown in Figure 2c. Firstly, THS was modified with the heterobifunctional linker maleimido trioxa-6-formyl benzamide (**1**), which reacts with the thiol groups through maleimide chemistry and introduces an aromatic aldehyde group linked to a hydrophilic di(ethylene glycol) spacer. All eight thiol groups present in THS could be modified with a 25-fold excess (with respect to thiol groups) of the linker, as determined by UV/Vis spectroscopy (see the Supporting Information). In a parallel step, the lysine groups of the fluorescent proteins were modified with a second heterobifunctional linker, succinimidyl 6-hydrazinonicotinate acetone hydrazone (**3**), which introduced a hydrazide functionality into the protein. An average of 2.1 of the 12 surface exposed lysine groups of the fluorescent proteins were modified with a 10-fold excess of reagent (see the Supporting Information).

The coupling between the modified THS and the modified fluorescent proteins was carried out by simple incubation of a mixture of the proteins for 16 h at room temperature in a coupling buffer at a THS concentration of $2\,mg\,mL^{-1}$. Addition of ATP to the reaction mixture did not improve the coupling ratio significantly, thus ATP was omitted in the experiments. The coupling product THS-eCFP-eYFP (**6**) was purified by size-exclusion chromatography. In order to be incorporated into polymeric materials, **6** was further modified with acrylamide groups by reaction with a 320-fold excess (relative to THS) of *N*-succinimidyl acrylate (**7**), followed by diafiltration to yield **8**.

Native PAGE of the hybrid **6** showed a fluorescent band where the assembled THS is expected to appear, which indicates that the fluorescent proteins were indeed encapsulated in the chaperonin (Figure 3a). TEM micrographs of the hybrid proved that the overall structure of THS remains intact (Figure 3b). The success of the coupling was quantified by UV/Vis spectroscopy, as the reaction between the two linkers yields a stable bisaryl hydrazone bond with a distinct absorption band in the UV region.[14] A typical spectrum of the purified host–guest hybrid is shown in Figure 3c. From the individual components of the composite spectrum, the coupling ratios were determined to be eCFP/THS = 0.44 ± 0.03, eYFP/THS = 0.71 ± 0.03 and (eCFP + eYFP)/THS = 1.15 ± 0.04. An average of 1.60 ± 0.06 hydrazone bonds were formed by each fluorescent protein. This data shows that the two fluorescent proteins are covalently entrapped inside the THS. The protein is most likely a mixed population of empty, singly, and doubly occupied THS, in which each cavity hosts no more than one fluorescent protein because of steric exclusion.

Fluorescence spectroscopy measurements proved that FRET occurs between the fluorescent proteins (Figure 3d and the Supporting Information). These results were confirmed and quantified by fluorescence lifetime imaging microscopy (FLIM) of the protein solution. FLIM represents a concentration- and cross-bleed-independent method to

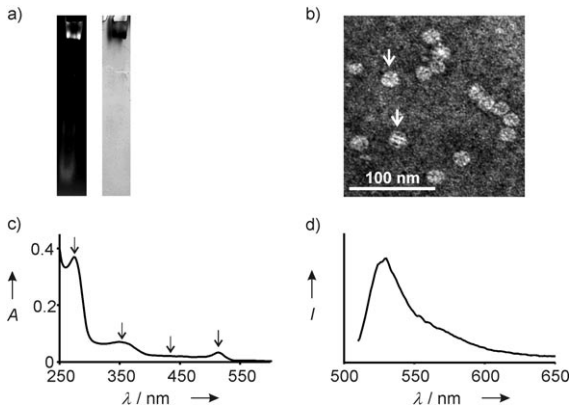

Figure 3. Analytical evidence for the successful synthesis of THS-eCFP-eYFP. a) Native PAGE of the purified sample. The gel was imaged in fluorescence mode (left) and subsequently stained with Coomassie Blue (right). b) TEM micrograph of the sample. Fully assembled THS complexes are visible in top and side views. A top view of a protein is highlighted by an arrow in the upper half of the image and a side view in the lower half. c) UV/Vis spectrum with arrows indicating components at 513 nm (eYFP), 439 nm (eCFP), 354 nm (bisaryl hydrazone linker), and 276 nm (THS, eCFP, and eYFP). d) Fluorescence emission spectrum of THS-eCFP-eYFP (excitation at wavelength of eCFP and corrected for spectral bleed-through) with the characteristics of an eYFP emission spectrum, thus proving FRET between eCFP and eYFP. (see the Supporting Information for the non-deconvoluted spectrum and the detailed protocol for how the spectrum shown was generated.)

detect and quantify FRET, because the decrease of the quantum yield of the donor as a result of FRET is accurately reported by a decrease of the donor lifetime (τ_{donor}).[11] The fluorescence decay trajectories of eCFP coencapsulated with eYFP in THS are clearly described by a double-exponential decay function (see the Supporting Information). A relatively short-lived component can be attributed to donor molecules that interact with the eYFP ($\tau_{donor} = (1.69 \pm 0.07)$ ns, occupancy $(56 \pm 3)\%$), and a longer-lived component ($\tau_{donor} = (2.75 \pm 0.06)$ ns, occupancy $(44 \pm 3)\%$) arises from noninteracting donor molecules. From the ratio of the lifetimes, an intermolecular distance of (5.23 ± 0.13) nm was determined. The mean lifetime was calculated to be $\tau_{mean} = (2.16 \pm 0.02)$ ns.

In order to synthesize protein–polymer hybrid materials, **8** (20.8 μg, that is, 0.8 μg of fluorescent proteins), acrylamide (10 mg), and the cross-linker *N*,*N*′-methylene-bis-acrylamide (0.1 mg) were dissolved in sodium phosphate buffer (40 μL, 50 mM; pH 7.4, 75 mM NaCl) and copolymerized by initiation with ammonium persulfate/tetramethylethylenediamine at room temperature. The resulting hydrogels were intensively extracted with buffer and water, and finally air dried at room temperature to give the transparent, fluorescent, and glassy polyacrylamide (PAAm).

These polymers were used as model systems to investigate the effect of mechanical deformation of the polymer on the biomechanical sensor. To this end, samples of the polymer were uniaxially strained until they fractured. The area surrounding the fracture face was imaged by multichannel confocal microscopy (Figure 4). The images clearly show the formation of microcracks arising from the applied strain. The

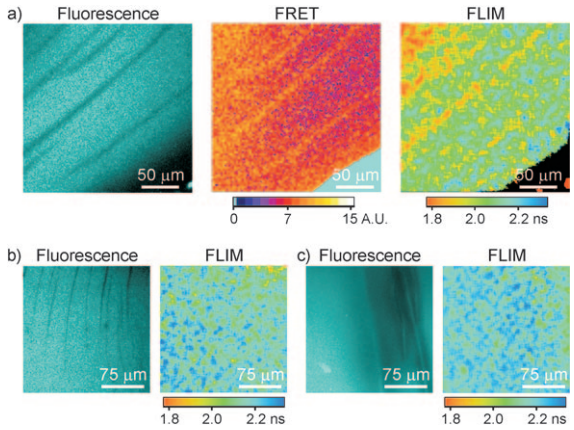

Figure 4. Confocal fluorescence microscopy analysis of strained and fractured PAAm-THS-eCFP-eYFP (a) and control experiments with strained and fractured PAAm-eCFP (b) and PAAm-THS-eCFP (c). The fluorescence emission in the blue channel upon excitation of eCFP, intensity-based FRET, and τ_{mean} value of the eCFP (calculated from FLIM) are shown.

FRET efficiency in the nondeformed material surrounding the cracks is surprisingly low. However, the FRET signal increases 1.5-fold in regions corresponding to the locations of the cracks. The FLIM images show a shorter mean lifetime of the donor within the cracks ($\tau_{mean} = (1.86 \pm 0.05)$ ns) compared to the surrounding matrix ($\tau_{mean} = (2.07 \pm 0.06)$ ns), which corresponds to a higher FRET efficiency. The lifetime difference suggests that changes in the microenvironment of the fluorophores within the cracks occurs, which most likely arises from a shortening of the donor–acceptor distance.

Thus, of the two reporting mechanisms depicted in Figure 1, the second is more likely; that is, THS-eCFP-eYFP reports the presence of cracks through relaxation of stress imposed during polymerization and subsequent drying of the PAAm. Upon application of strain, the formation of cracks and their propagation is accompanied by a plastic deformation of the polymer at the crack tip. As the crack propagates, it leaves behind a strip of deformed material. The plastic deformation allows the polymer chains and the attached sensor proteins at the crack edges to relax, which results in an increased FRET signal that remains narrow even for long cracks. While this explanation is no doubt a simplification of what actually takes place within the heterogeneous PAAm network, it is consistent with both the FRET and FLIM images.

Control experiments were carried out with AAm that was copolymerized with acrylamide-modified eCFP (Figure 4b) or a thermosome encapsulating eCFP alone (Figure 4c). These polymers fluoresce, but, as expected, do not exhibit a FRET signal. Straining of these polymers leads to microcrack formation and fracture. The cracks are visible in the fluorescence image as dark regions. However, in the FLIM images, no significant difference between the undamaged matrix and the crack regions was detected (PAAm-eCFP: $\tau_{mean}(crack) = (2.05 \pm 0.09)$ ns, $\tau_{mean}(matrix) = (2.15 \pm 0.05)$ ns; PAAm-THS-eCFP: $\tau_{mean}(crack) = (2.17 \pm 0.07)$ ns, $\tau_{mean}(matrix) = (2.19 \pm 0.04)$ ns), which indicates that the THS-eCFP-eYFP construct is essential for the FRET detection of localized mechanical deformation of the polymer.

In conclusion, we report a polymer–protein hybrid material in which changes in stress of the polymer matrix result in changes to the fluorescence properties of the protein complex, thus creating a material that visually reports damage. Further work is underway to examine the sensitivity of the sensor. Ideally, it will be able to report damage on a submicrometer scale before visible cracks become detectable by standard microscopic methods. These self-reporting materials could be used in myriad applications where easy and early detection of damage is essential to avoid catastrophic failure of the material.

Received: January 29, 2009
Published online: April 28, 2009

Keywords: FRET · hybrid materials · polymers · proteins · stress detection

[1] D. W. P. M. Löwik, L. Ayres, J. M. Smeek, J. C. M. Van Hest, *Adv. Polym. Sci.* **2006**, *202*, 19–52.
[2] a) P. Wang, M. V. Sergeeva, L. Lim, J. S. Dordick, *Nat. Biotechnol.* **1997**, *15*, 789–793; b) I. Gill, A. Ballesteros, *Trends Biotechnol.* **2000**, *18*, 469–479; c) N. Bruns, J. C. Tiller, *Nano Lett.* **2005**, *5*, 45–48.
[3] a) K. E. LeJeune, A. J. Russell, *Biotechnol. Bioeng.* **1996**, *51*, 450–457; b) K. E. LeJeune, J. R. Wild, A. J. Russell, *Nature* **1998**, *395*, 27–28; c) I. Gill, A. Ballesteros, *Biotechnol. Bioeng.* **2000**, *70*, 400–410; d) A. J. Russell, J. A. Berberich, G. E. Drevon, R. R. Koepsel, *Annu. Rev. Biomed. Eng.* **2003**, *5*, 1–27.
[4] C. Wang, R. J. Stewart, J. Kopecek, *Nature* **1999**, *397*, 417–420.
[5] W. L. Murphy, W. S. Dillmore, J. Modica, M. Mrksich, *Angew. Chem.* **2007**, *119*, 3126–3129; *Angew. Chem. Int. Ed.* **2007**, *46*, 3066–3069.
[6] a) D. Tada, T. Tanabe, A. Rachibana, K. Yamauchi, *J. Biosci. Bioeng.* **2005**, *100*, 551–555; b) A. P. Esser-Kahn, M. B. Francis, *Angew. Chem.* **2008**, *120*, 3811–3814; *Angew. Chem. Int. Ed.* **2008**, *47*, 3751–3754.
[7] a) M. Motuku, U. K. Vaidya, G. M. Janowski, *Smart Mater. Struct.* **1999**, *8*, 623–638; b) S. M. Bleay, C. B. Loader, V. J. Hawyes, L. Humberstone, P. T. Curtis, *Composites Part A* **2001**, *32*, 1767–1776; c) J. W. C. Pang, I. P. Bond, *Composites Part A* **2005**, *36*, 183–188; d) J. W. C. Pang, I. P. Bond, *Compos. Sci. Technol.* **2005**, *65*, 1791–1799; e) S. D. Bergman, F. Wudl, *J. Mater. Chem.* **2008**, *18*, 41–62.
[8] L. Ditzel, J. Löwe, D. Stock, K.-O. Stetter, H. Huber, R. Huber, S. Steinbacher, *Cell* **1998**, *93*, 125–138.
[9] F. Valle, J. A. DeRose, G. Dietler, M. Kawe, A. Plückthun, G. Semeza, *Ultramicroscopy* **2002**, *93*, 83–89.
[10] a) F. U. Hartl, M. Hayer-Hartl, *Science* **2002**, *295*, 1852–1858; b) S. Walter, J. Buchner, *Angew. Chem.* **2002**, *114*, 1142–1158; *Angew. Chem. Int. Ed.* **2002**, *41*, 1098–1113; c) A. L. Horwich, G. W. Farr, W. A. Fenton, *Chem. Rev.* **2006**, *106*, 1917–1930.
[11] M. A. Rizzo, G. Springer, K. Segawa, W. R. Zipfel, D. W. Piston, *Microsc. Microanal.* **2006**, *12*, 238–254.
[12] D. W. Piston, G.-J. Kremers, *Trends Biochem. Sci.* **2007**, *32*, 407–414.
[13] M. G. Bigotti, A. R. Clarke, *J. Mol. Biol.* **2005**, *348*, 13–26.
[14] G. T. Hermanson, *Bioconjugate Techniques*, 2nd ed., Academic Press, London, **2008**, p. 730.

